Figure S1

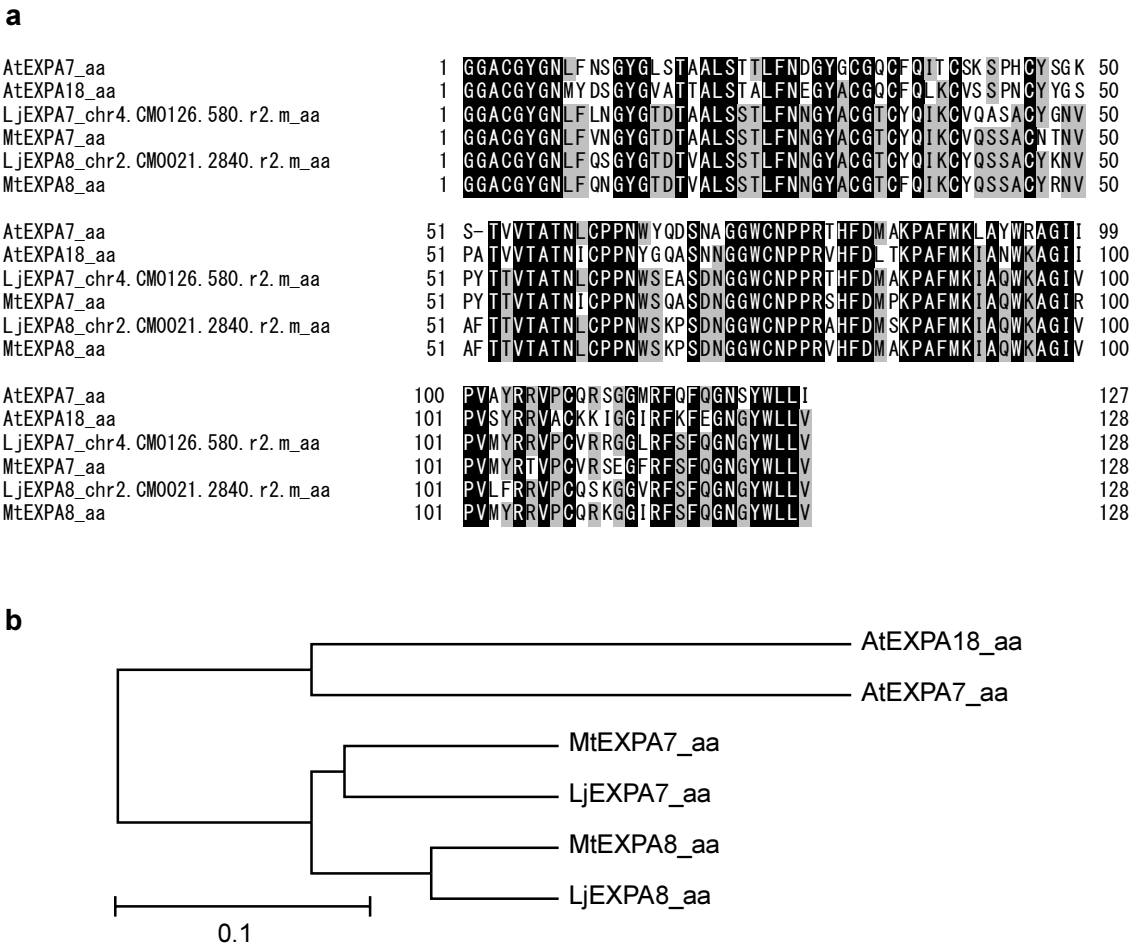

Figure S1
The multiple alignment of expansin protein sequences by CLUSTAL W.
(**a**) The amino acid sequence between 55 (as “1” in the illustration) and 181 (as “127” in the illustration) of AtEXPA7 and the equivalent regions of each expansin protein sequence were aligned by CLUSTAL W. Residues that are identical among all amino acid sequences (black) and conserved substitutions (gray) are indicated. (**b**) Phylogenetic tree based on the amino acid sequence between 55 (Gly) and 181 (Ile) of AtEXPA7 and the equivalent regions of each expansin protein sequence.

Figure S2

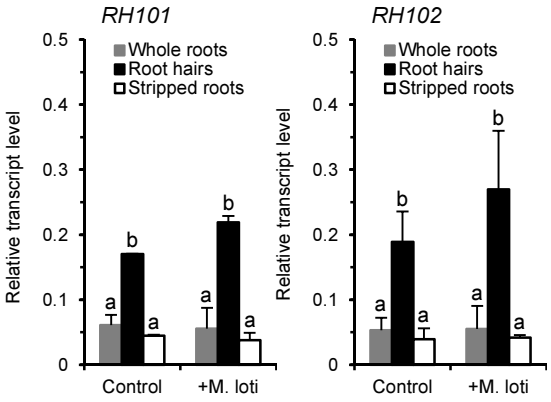

Figure S2
Root hair-specific expression analysis of *RH101* and *RH102* in response to infection by *M. loti*.
Real-time RT-PCR analysis of *RH101* and *RH102* transcripts in root hair cells, stripped roots or whole roots 2 days after mock-inoculation (Control) or inoculation with *M. loti* (+M. loti). The data are indicated as means and SD of 3 or 4 biological replications. Means with different letters are significantly different (Tukey-Kramer multiple comparison test, $P<0.05$).

Figure S3

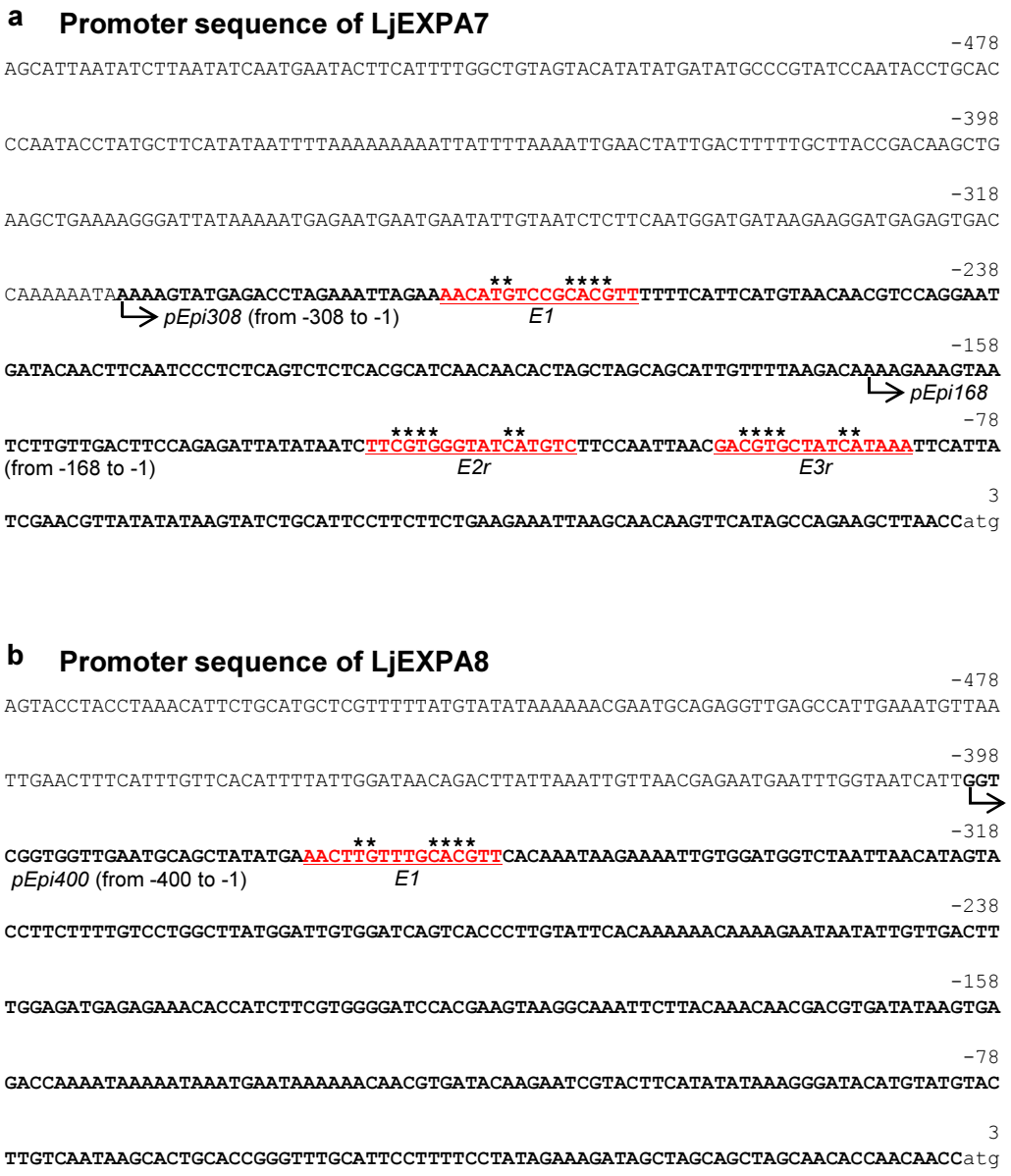

Figure S3
Promoter sequences of LjEXP7 and LjEXPA8.
The promoter sequences of LjEXPA7 and LjEXPA8 from -557 to +3 are shown in (**a**) and (**b**), respectively. The transcriptional start site is designated +1. Red underlined nucleotide sequences represent putative root hair-specific *cis* elements (RHE) cores located within the promoter sequences of LjEXPA7 and LjEXPA8. Highly conserved nucleotides within the RHE core are denoted by asterisks. An "r" of E2r and E3r indicates a reverse orientation of the RHE. Bold nucleotide sequences below the arrows show sequences of three types of RHEs-containing promoters, *pEpi168* (from -168 to -1), *pEpi308* (from -308 to -1) and *pEpi400* (from -400 to -1).

Figure S4

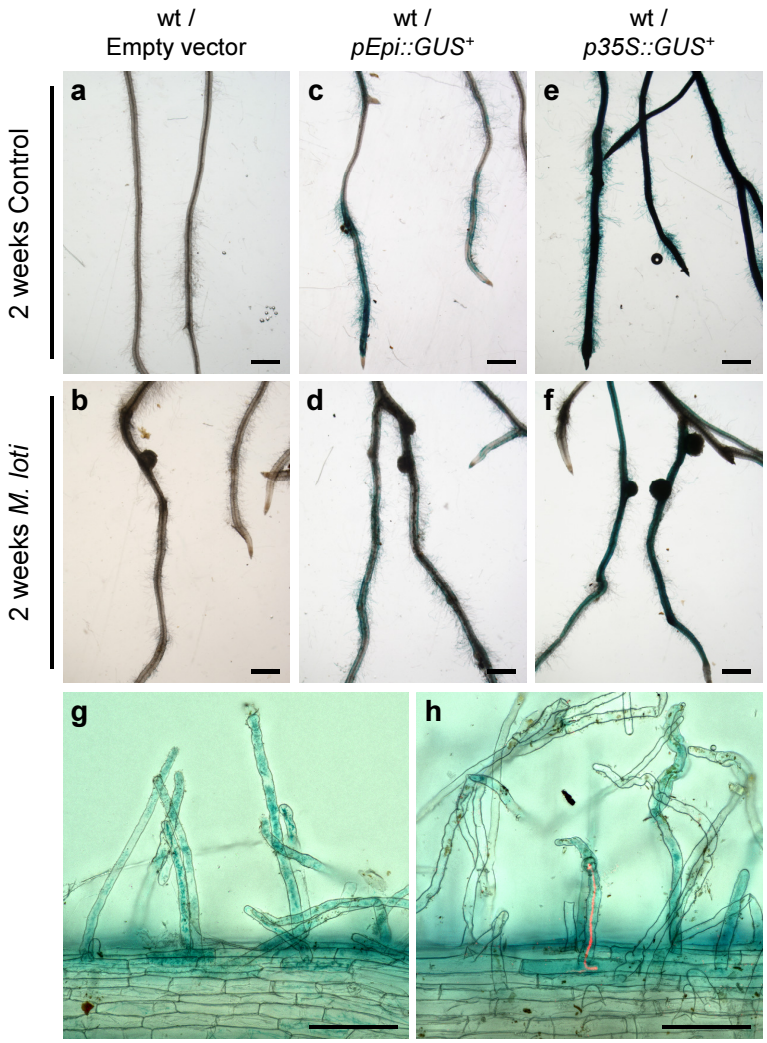

Figure S4
Histochemical localization of GUS activity in wt roots transformed with *pEpi::GUS*⁺ vector.
(**a**-**f**) Bright-field images of X-Gluc incubated wt roots transformed with an empty vector control (Empty vector) (**a**, **b**), *pEpi::GUS*⁺ (*pEpi::GUS*⁺) (**c**, **d**) and *p35S::GUS*⁺ (**e**, **f**) vectors. Expression patterns of *GUS*⁺ gene from transformed roots were observed 2 weeks after mock-inoculation (Control) (**a**, **c**, **e**) or inoculation with DsRed-labeled *M. loti* (**b**, **d**, **f**). (**g**, **h**) Root hairs of wt/*pEpi::GUS*⁺ roots observed 7 days after mock-inoculation (**g**) or inoculation with DsRed-labeled *M. loti* (**h**). Bright-field and red fluorescence images were merged into single images. (**h**) ITs can be seen inside the curled and GUS-stained root hairs. Scale bars are 1 mm (**a**-**f**) and 100 µm (**g**, **h**).

Figure S5

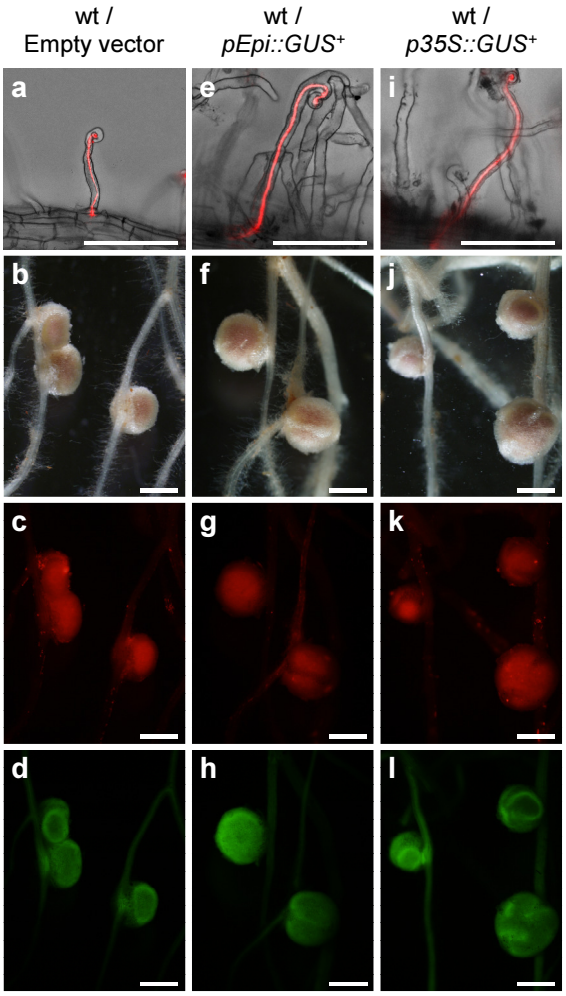

Figure S5
Rhizobial infection and nodule organogenesis phenotypes of wt roots transformed with *pEpi::GUS*⁺ vector.
(**a**-**l**) Symbiotic phenotypes of transformed wt roots were observed 4 weeks after inoculation with DsRed-labeled *M. loti*. Root phenotypes of wt/Empty vector (**a**-**d**), wt/*pEpi::GUS*⁺ (**e**-**h**), and wt/*p35S::GUS*⁺ (**i**-**l**). (**a**, **e**, **i**) ITs can be seen inside the curled root hairs, shown as merged images of bright-field and red fluorescence images. Bright-field images (**b**, **f**, **j**) and their corresponding red (**c**, **g**, **k**) and green (**d**, **h**, **l**) fluorescence images of nodulation phenotypes are shown. Nodules formed on the roots of wt/Empty vector (**b**-**d**), wt/*pEpi::GUS*⁺ (**f**-**h**) and wt/*p35S::GUS*⁺ (**j**-**l**). (**c**, **g**, **k**) Infection of DsRed-labeled *M. loti* was observed as red fluorescence in the central zone of nodules on those roots. (**d**, **h**, **l**) Green fluorescence as a transgenic marker is shown. Scale bars are 100 μm (**a**, **e**, **i**) and 1 mm (**b**-**d**, **f**-**h**, **j**-**l**).

Figure S6

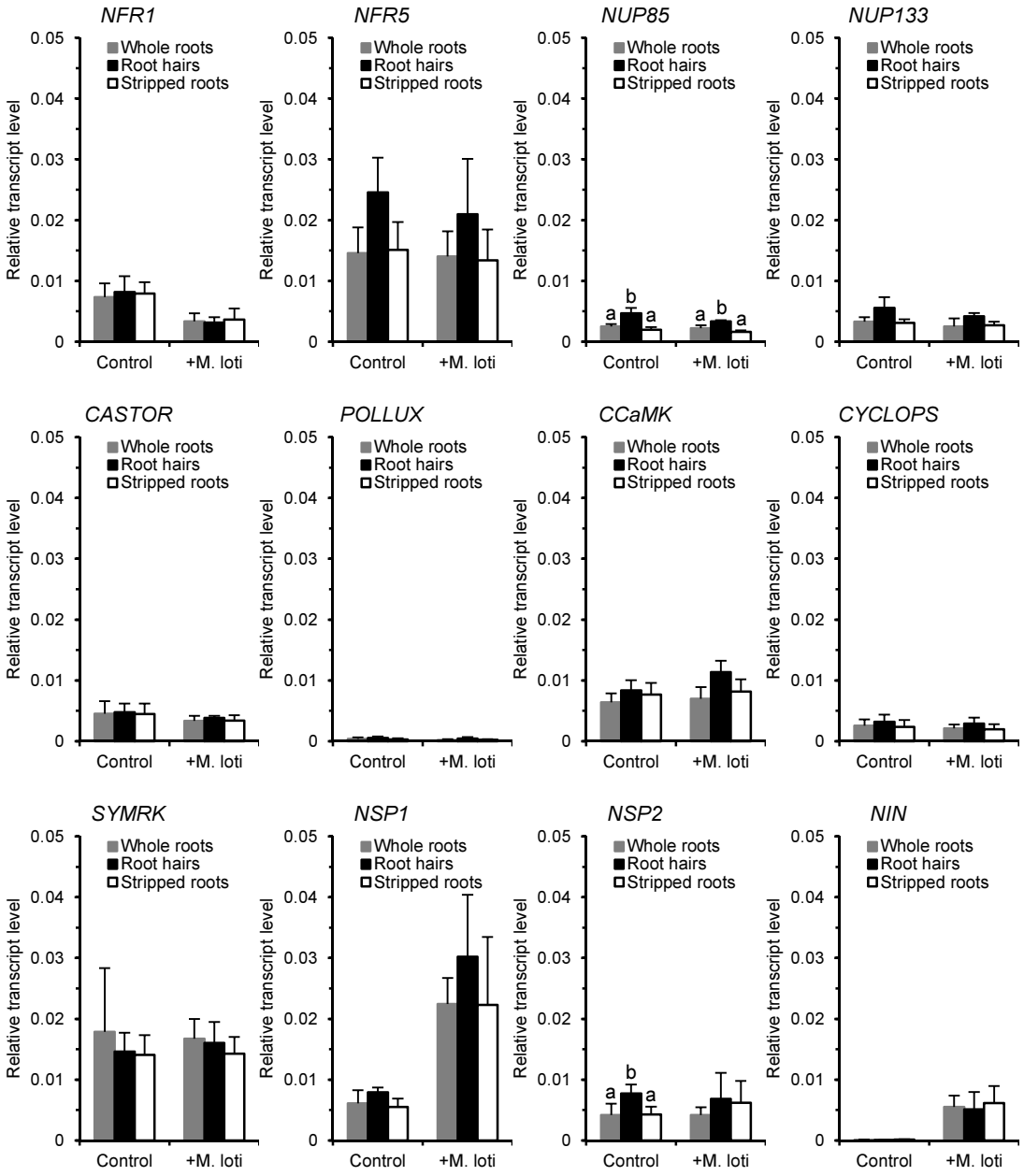

Figure S6

Expression analysis of symbiosis genes in root hairs, stripped roots and whole roots of *L. japonicus.*

Real-time RT-PCR analysis of *NFR1*, *NFR5*, *NUP85*, *NUP133*, *CASTOR*, *POLLUX*, *CCaMK*, *CYCLOPS*, *SYMRK*, *NSP1*, *NSP2* and *NIN* transcripts in root hairs, stripped roots or whole roots 2 days after mock-inoculation (Control) or inoculation with *M. loti* (+M. loti). The data are indicated as means and SD of 3 or 4 biological replications. Means with different letters are significantly different (Tukey-Kramer multiple comparison test, $P<0.05$).

Figure S7

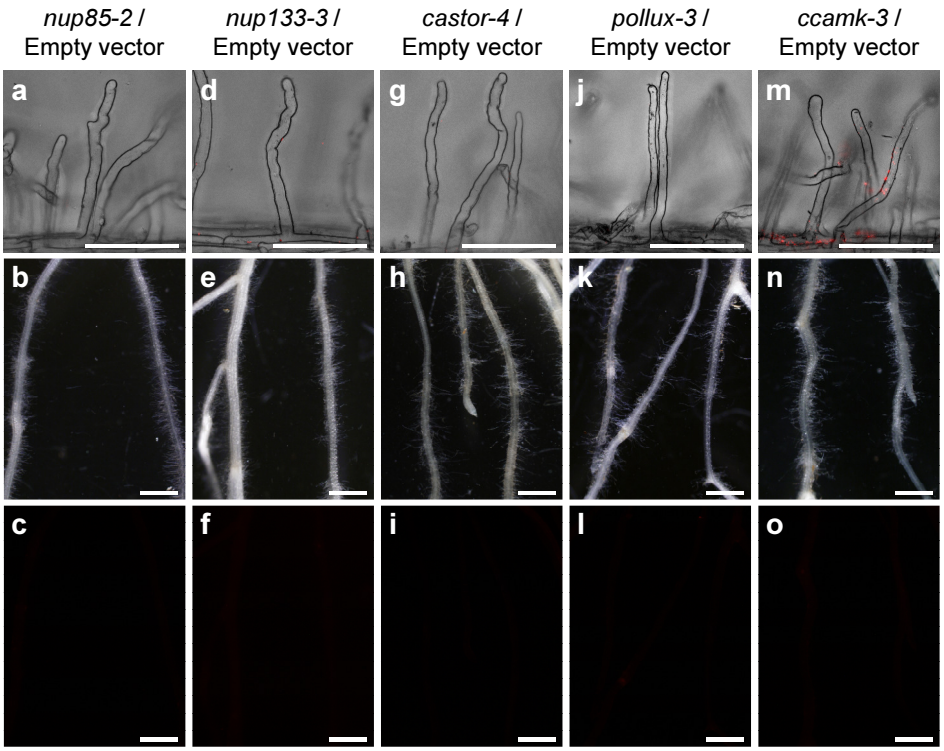

Figure S7
Rhizobial infection and nodule organogenesis phenotypes of *nup85-2*, *nup133-3*, *castor-4*, *pollux-3* and *ccamk-3* mutant roots transformed with an empty vector control.
(**a**-**o**) Symbiotic phenotypes of transformed non-nodulating mutant roots were observed 4 weeks after inoculation with DsRed-labeled *M. loti*. Root phenotypes of *nup85-2*/Empty vector (**a**-**c**), *nup133-3*/Empty vector (**d**-**f**), *castor-4*/Empty vector (**g**-**i**), *pollux-3*/Empty vector (**j**-**l**) and *ccamk-3*/Empty vector (**m**-**o**). (**a**, **d**, **g**, **j**, **m**) Neither bacterial colonization nor IT formation was observed; however, we show bright-field and red fluorescence images merged into single images. Bright-field images (**b**, **e**, **h**, **k**, **n**) and their corresponding red fluorescence images (**c**, **f**, **i**, **l**, **o**) of nodulation phenotypes are shown. Cortical cell division did not occur in the roots of *nup85-2*/Empty vector (**b**, **c**), *nup133-3*/Empty vector (**e**, **f**), *castor-4*/Empty vector (**h**, **i**), *pollux-3*/Empty vector (**k**, **l**) and *ccamk-3*/Empty vector (**n**, **o**). Scale bars are 100 μm (**a**, **d**, **g**, **j**, **m**) and 1 mm (**b**, **c**, **e**, **f**, **h**, **i**, **k**, **l**, **n**, **o**).

Figure S8

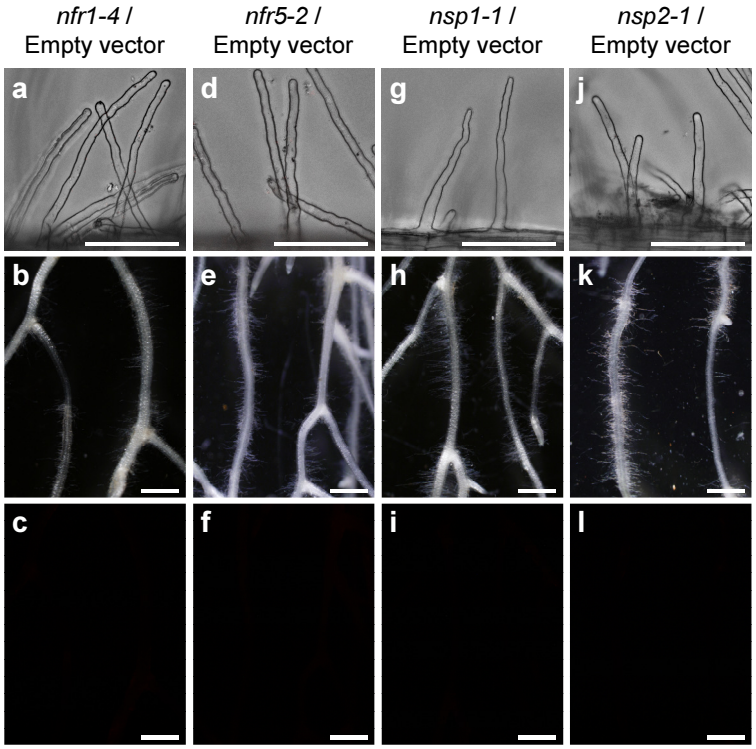

Figure S8
Rhizobial infection and nodule organogenesis phenotypes of *nfr1-4*, *nfr5-2, nsp1-1* and *nsp2-1* mutant roots transformed with an empty vector control.
(**a**-**l**) Symbiotic phenotypes of transformed non-nodulating mutant roots were observed 4 weeks after inoculation with DsRed-labeled *M. loti*. (**a**, **d**, **g**, **j**) Bright-field and red fluorescence images merged into single images. Neither bacterial colonization nor IT formation was observed on the roots of *nfr1-4*/Empty vector (**a**), *nfr5-2*/Empty vector (**d**), *nsp1-1*/Empty vector (**g**) and *nsp2-1*/Empty vector (**j**). Bright-field images (**b**, **e**, **h**, **k**) and their corresponding red fluorescence images (**c**, **f**, **i**, **l**) of nodulation phenotypes are shown. Cortical cell division did not occur in the roots of *nfr1-4*/Empty vector (**b**, **c**), *nfr5-2*/Empty vector (**e**, **f**), *nsp1-1*/Empty vector (**h**, **i**) and *nsp2-1*/Empty vector (**k**, **l**). Scale bars are 100 μm (**a**, **d**, **g**, **j**) and 1 mm (**b**, **c**, **e**, **f**, **h**, **i**, **k**, **l**).

Figure S9

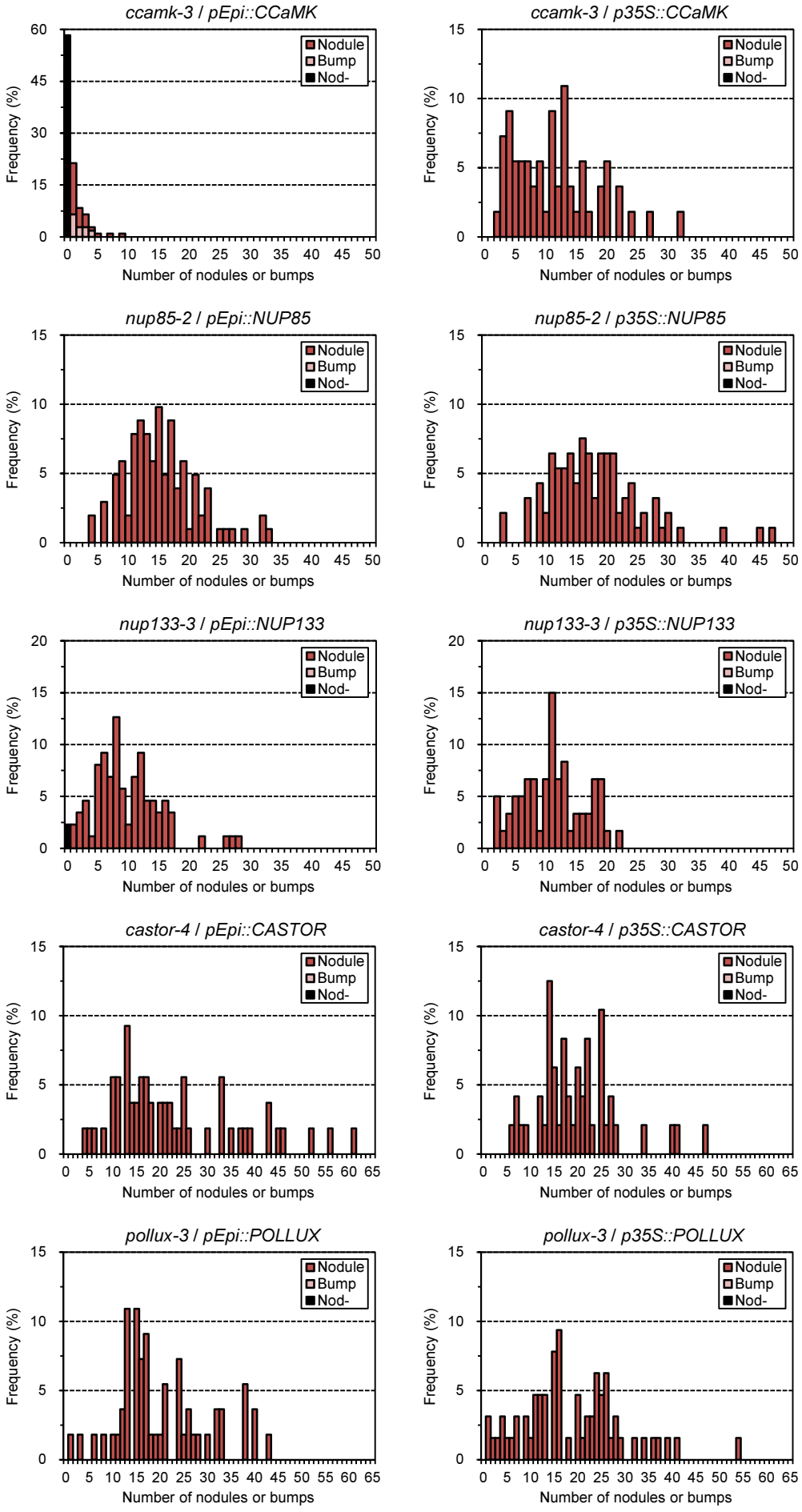
ccamk-3 / pEpi::CCaMK
ccamk-3 / p35S::CCaMK
nup85-2 / pEpi::NUP85
nup85-2 / p35S::NUP85
nup133-3 / pEpi::NUP133
nup133-3 / p35S::NUP133
castor-4 / pEpi::CASTOR
castor-4 / p35S::CASTOR
pollux-3 / pEpi::POLLUX
pollux-3 / p35S::POLLUX
Nodule
Bump
Nod-
Frequency (%)
Number of nodules or bumps

Figure S9

Stacked histograms comparing frequency counts in terms of the number of nodules or bumps per mutant plants transformed with *CCaMK*, *CASTOR*, *POLLUX*, *NUP85* and *NUP133* driven by *pEpi* or *p35S*.

Black bar, positioned at x=0, represents the frequency of non-nodulating plants per total plants examined (Nod^-). X-axis; the number of nodules or bumps/plant. Y-axis; frequency of non-nodulation (black), bump-formed (pink) or nodulated (red) plants.

Figure S10

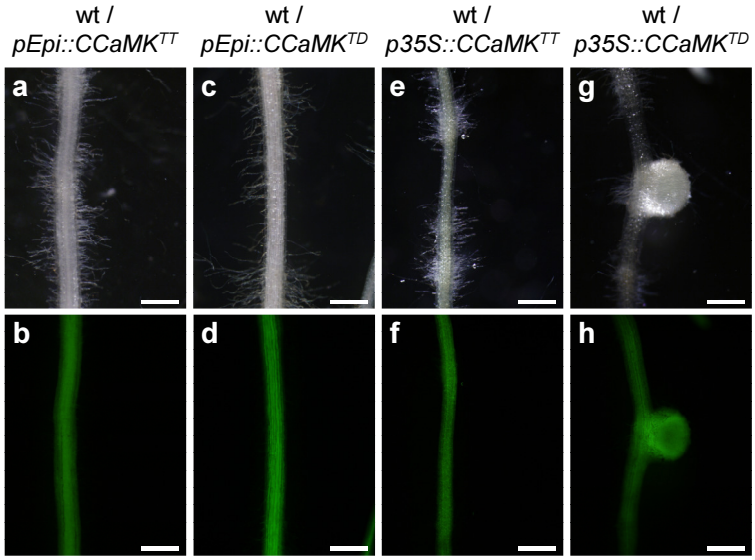

Figure S10
Spontaneous nodulation phenotypes of wt roots transformed with *CCaMK^{T265D}* driven by *pEpi* or *p35S*.
(**a**-**h**) Introduction of gain-of-function CCaMK^{T265D} (CCaMK^{TD}) under the control of *p35S* could induce spontaneous nodulation in the absence of rhizobia (**g**, **h**). However, on the roots of wt/*pEpi308::CCaMK^{T265D}* (wt/*pEpi::CCaMK^{TD}*) (**c**, **d**) as well as those of wt/*pEpi308::CCaMK^{T265T}* (wt/*pEpi::CCaMK^{TT}*) (**a**, **b**) and wt/*p35S::CCaMK^{T265T}* (wt/*p35S::CCaMK^{TT}*) (**e**, **f**), spontaneous nodulation did not occur even 6 weeks after transplantation. Green fluorescence as a transgenic marker is shown (**b**, **d**, **f**, **h**). Scale bars are 1 mm (**a**-**h**).

Figure S11

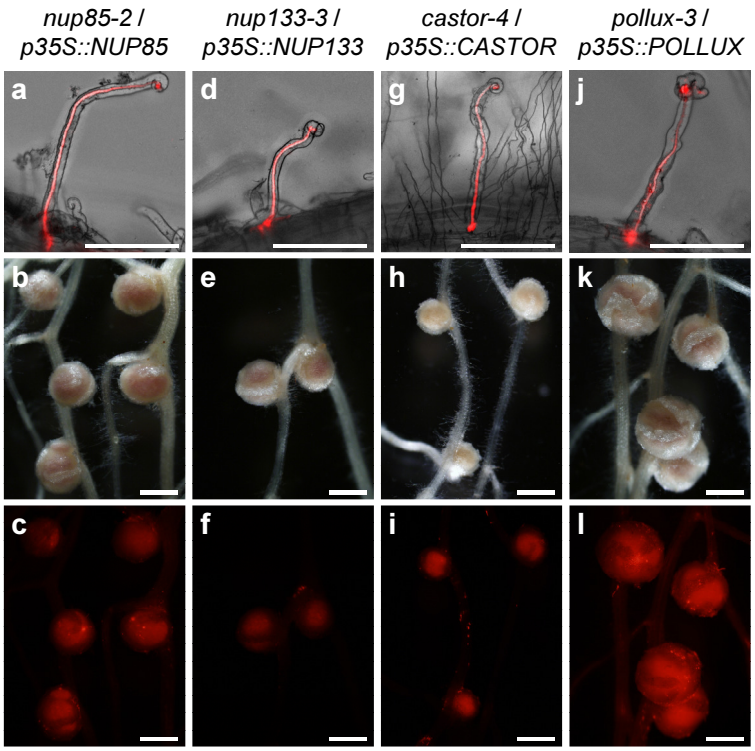

Figure S11
Complementation tests of rhizobial infection and nodule organogenesis phenotypes of *nup85-2*, *nup133-3*, *castor-4* and *pollux-3* mutants transformed with the corresponding genes driven by *p35S*.
(**a**-**l**) Symbiotic phenotypes of transformed roots were observed 4 weeks after inoculation with DsRed-labeled *M. loti*. Root phenotypes of *nup85-2/pEpi::NUP85* (**a**-**c**), *nup133-3/pEpi::NUP133* (**d**-**f**), *castor-4/p35S::CASTOR* (**g**-**i**) and *pollux-3/p35S::POLLUX* (**j**-**l**). (**a**, **d**, **g**, **j**) ITs can be seen inside the curled root hairs, shown as merged images of bright-field and red fluorescence images. Bright-field images (**b**, **e**, **h**, **k**) and their corresponding red fluorescence images (**c**, **f**, **i**, **l**) of nodulation phenotypes are shown. (**c**, **f**, **i**, **l**) Infection of DsRed-labeled *M. loti* was observed as red fluorescence in the central zone of nodules. Scale bars are 100 μm (**a**, **d**, **g**, **j**) and 1 mm (**b**, **c**, **e**, **f**, **h**, **i**, **k**, **l**).

Figure S12

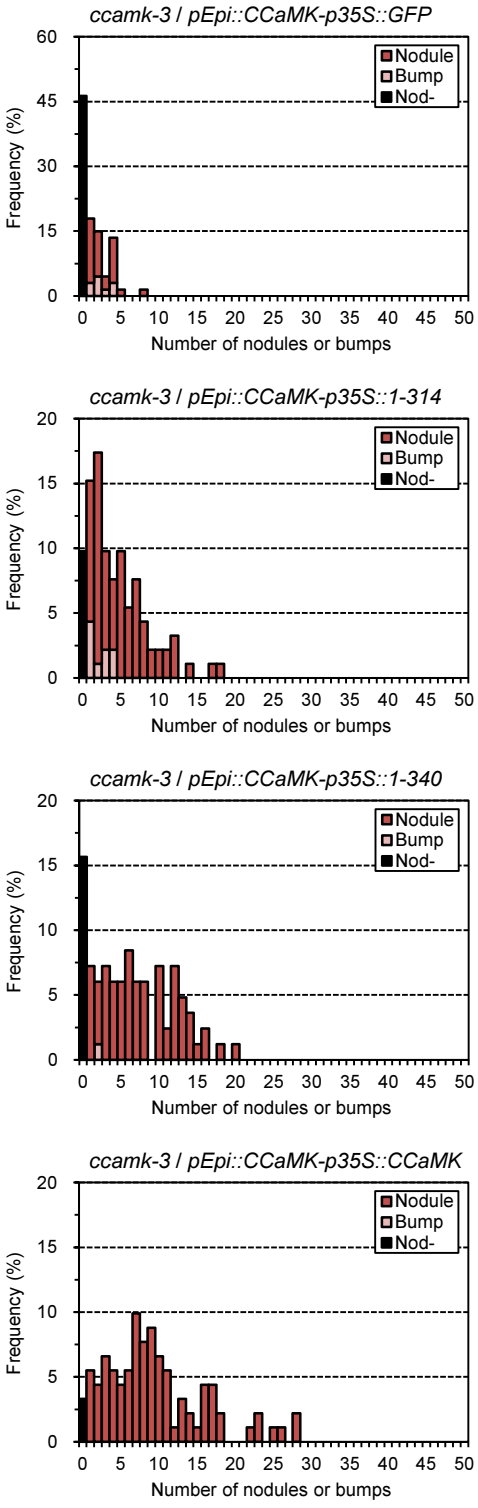

Figure S12
Stacked histograms comparing frequency counts in terms of the number of nodules or bumps per mutant plant by co-transformation with *CCaMK* under the control of *pEpi* and truncated *CCaMK1-314* or *CCaMK1-340* under the control of *p35S*.
Black bar, positioned at x=0, represents the frequency of non-nodulating plants per total plants examined (Nod^-). X-axis; the number of nodules or bumps/plant. Y-axis; frequency of non-nodulation (black), bump-formed (pink) or nodulated (red) plants.

Figure S13

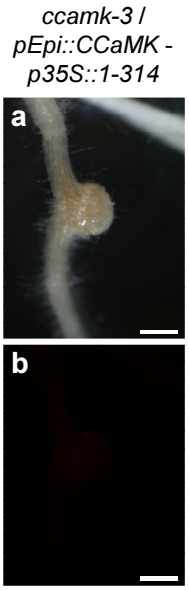

Figure S13
Spontaneous nodule-like structure of *ccamk-3* mutant by co-transformation with *CCaMK* under the control of *pEpi* and a truncated *CCaMK1-314* under the control of *p35S*.
(**a**, **b**) Nodulation phenotypes of transformed roots were observed 4 weeks after inoculation with DsRed-labeled *M. loti*. Bright-field image (**a**) and the corresponding red fluorescence image (**b**) of nodulation phenotypes are shown. In addition to infected nodules as shown in Figure 4, spontaneous nodule-like structures without rhizobial infection were also formed on the roots of *ccamk-3/pEpi::CCaMK-p35S::CCaMK1-314* (**a**, **b**). Scale bars are 1 mm (**a**, **b**).

Figure S14

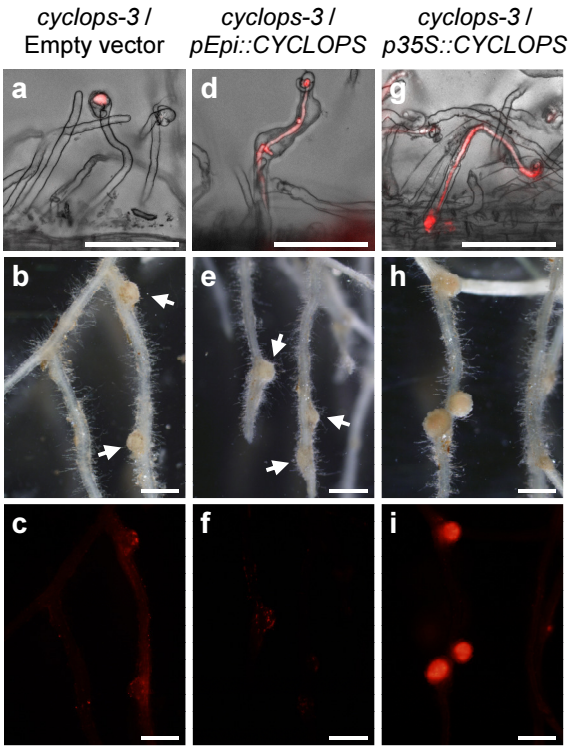

Figure S14
Complementation tests of rhizobial infection and nodule organogenesis phenotypes of *cyclops-3* mutants transformed with *CYCLOPS* driven by *pEpi* or *p35S*.
(**a**-**i**) Symbiotic phenotypes of transformed roots were observed 4 weeks after inoculation with DsRed-labeled *M. loti*. Root phenotypes of *cyclops-3*/Empty vector (**a**-**c**), *cyclops-3*/*pEpi::CYCLOPS* (**d**-**f**) and *cyclops-3*/*p35S::CYCLOPS* (**g**-**i**). Micro-colony (**a**) or ITs can be seen inside the curled root hairs (**d**, **g**), shown as merged images of bright-field and red fluorescence images. Bright-field images (**b**, **e**, **h**) and their corresponding red fluorescence images (**c**, **f**, **i**) of nodulation phenotypes are shown. On the roots of *cyclops-3*/Empty vector, though deformation of root hairs and colonization of bacteria in curled root hairs were observed, development of ITs within the root hairs did not occur (**a**). Cortical cell division arrested at bump structure (arrows in **b**). On the roots of *cyclops-3*/*pEpi::CYCLOPS*, epidermal IT formation was recovered (**d**), while cortical cell division was not coupled with IT penetration, resulting in the formation of bumps (arrows in **e**). (**h**, **i**) Nodules formed on the roots of *cyclops-3*/*p35S::CYCLOPS*. Infection of DsRed-labeled *M. loti* was observed as red fluorescence in the central zone of nodules (**i**). Scale bars are 100 μm (**a**, **d**, **g**) and 1 mm (**b**, **c**, **e**, **f**, **h**, **i**).

Figure S15

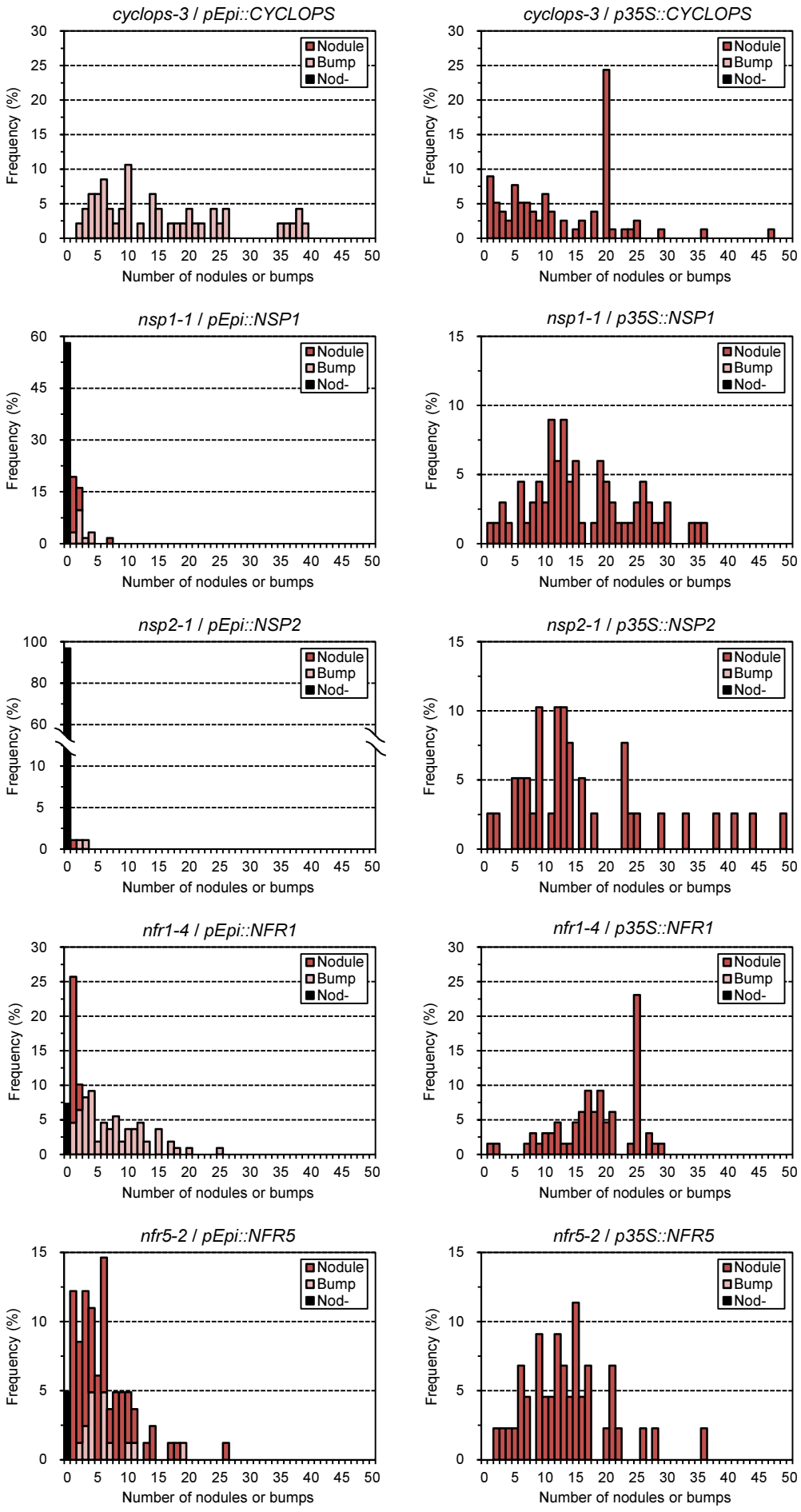
cyclops-3 / pEpi::CYCLOPS
cyclops-3 / p35S::CYCLOPS
nsp1-1 / pEpi::NSP1
nsp1-1 / p35S::NSP1
nsp2-1 / pEpi::NSP2
nsp2-1 / p35S::NSP2
nfr1-4 / pEpi::NFR1
nfr1-4 / p35S::NFR1
nfr5-2 / pEpi::NFR5
nfr5-2 / p35S::NFR5
Nodule
Bump
Nod-
Frequency (%)
Number of nodules or bumps

Figure S15

Stacked histograms comparing frequency counts in terms of the number of nodules or bumps per mutant plant transformed with *CYCLOPS*, *NSP1*, *NSP2*, *NFR1* and *NFR5* driven by *pEpi* or *p35S*.

Black bar, positioned at x=0, represents the frequency of non-nodulating plant per total plants examined (Nod^-). X-axis; the number of nodules or bumps/plant. Y-axis; frequency of non-nodulation (black), bump-formed (pink) or nodulated (red) plants.

Figure S16

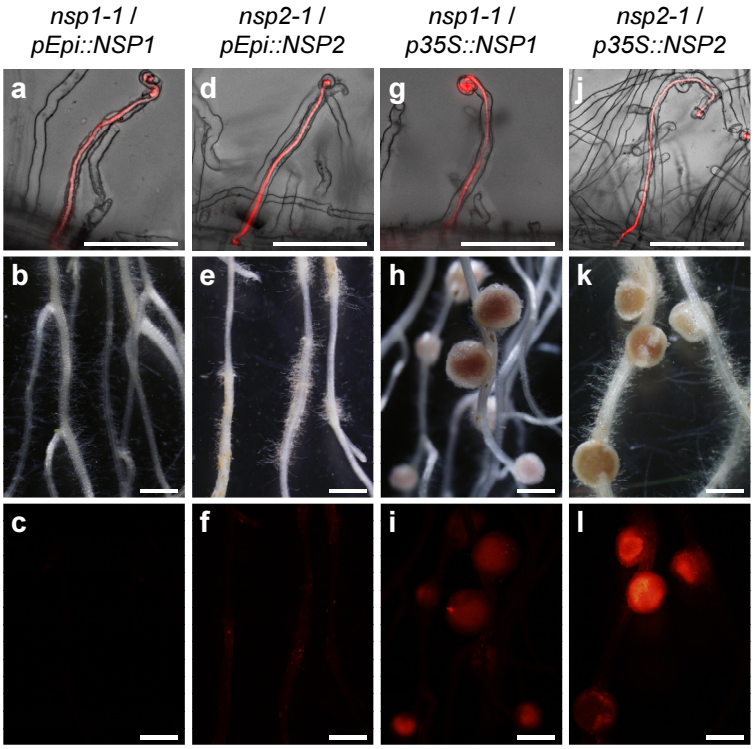

Figure S16
Complementation tests of rhizobial infection and nodule organogenesis phenotypes of *nsp1-1* and *nsp2-1* mutants transformed with the corresponding genes driven by *pEpi* or *p35S*.
(**a**-**l**) Symbiotic phenotypes of transformed roots were observed 4 weeks after inoculation with DsRed-labeled *M. loti*. Root phenotypes of *nsp1-1*/*pEpi::NSP1* (**a**-**c**), *nsp2-1*/*pEpi::NSP2* (**d**-**f**), *nsp1-1*/*p35S::NSP1* (**g**-**i**) and *nsp2-1*/*p35S::NSP2* (**j**-**l**). (**a**, **d**, **g**, **j**) ITs can be seen inside the curled root hairs, shown as merged images of bright-field and red fluorescence images. Bright-field images (**b**, **e**, **h**, **k**) and their corresponding red fluorescence images (**c**, **f**, **i**, **l**) of nodulation phenotypes are shown. Nodules formed on the roots of *nsp1-1*/*p35S::NSP1* (**h**, **i**) and *nsp2-1*/*p35S::NSP2* (**k**, **l**). (**i**, **l**) Infection of DsRed-labeled *M. loti* was observed as red fluorescence in the central zone of nodules. Nodule organogenesis was not induced on the roots of *nsp1-1*/*pEpi::NSP1* (**b**, **c**) and *nsp2-1*/*pEpi::NSP2* (**e**, **f**). Scale bars are 100 μm (**a**, **d**, **g**, **j**) and 1 mm (**b**, **c**, **e**, **f**, **h**, **i**, **k**, **l**).